

Supplementary Information

Performance of Composite Oxygen Carriers for Plasma-Assisted Nitrogen Fixation and Ammonia Synthesis

Baiqiang Zhang*¹, Yongqi Liang¹, Jia Wang¹, Xi Chen¹, Anqi Li¹, Yuyang Zhang¹, Yuhui Chen¹, Shiquan Zhu¹, Nobusuke Kobayashi², Bo Wu*³

1 Henan International Joint Laboratory of Energy Efficient Conversion and Utilization, School of Energy and Power Engineering, Zhengzhou University of Light Industry, PR China

2 Environmental and Renewable Energy Systems, Gifu University, Japan

3 Engineering Research Center of Advanced Functional Material Manufacturing of Ministry of Education, School of Ecology and Environment, Zhengzhou University, PR China

* Corresponding author. E-mail address: zbq415@gmail.com (Baiqiang Zhang), wb@zzu.edu.cn (Bo Wu)

Table of Contents

S.1 Analysis of Plasma Discharge Temperature Characteristics **S1**

Fig. S1 Thermal imaging diagram of the reactor during the 97%-TiMgO plasma nitrogen fixation process.

S.2 Thermodynamic calculation **S2**

Fig. S2 ΔG variation with temperature. (a) Nitrogen fixation reaction, (b) Nitrogen release reaction.

Tab. S1 Comparison of hydrolysis characteristics of metal nitrides.

S.3 Characterization analysis **S3**

Fig. S3 XRD patterns of the MO_x before the reaction.

Fig. S4 SEM images of (a) 97wt%-TiMgO (F), (b) 97wt%-TiMgO (P), (c) 9wt%-ZrMgO (F), (d) 9wt%-ZrMgO (P). Scale bars: 1 μm . F and P denote fresh and post-reaction samples, respectively.

Fig. S5 XPS full spectra of 9 wt%-TiMgO and 97 wt%-TiMgO.

Fig. S6 Mg 1s spectra of (a) 9 wt%-TiMgO, (b) 97 wt%-TiMgO.

Fig. S7 Ti 2p spectra of (a) 9 wt%-TiMgO, (b) 97 wt%-TiMgO.

Tab. S2. XPS N 1s quantification of nitrogen species during F(fresh)、P(plasma nitrated) and H(hydrolyzed).

Fig. S8 XPS full spectra of 9 wt%-ZrMgO and 97 wt%-ZrMgO.

Fig. S9 Mg 1s spectra of (a) 9 wt%-ZrMgO, (b) 97 wt%-ZrMgO.

Fig. S10 O 1s spectra of (a) 9 wt%-ZrMgO, (b) 97 wt%-ZrMgO.

Fig. S11 Zr 3d spectra of (a) 9 wt%-ZrMgO, (b) 97 wt%-ZrMgO.

Tab. S3 Surface elemental distribution of 9 wt %-ZrMgO(P).

Fig. S12 Total number of elemental distribution spectra for 9 wt%-ZrMgO (P).

Tab. S4 Surface elemental distribution of 9 wt %-ZrMgO(P).

Fig. S13 EDS spot scanning of 9 wt%-ZrMgO.

S.4 Plasma spectral analysis **S9**

Fig. S14 OES spectra of MO_x after 15 min treatment.

Fig. S15 N_2 bands (a) at 5 minutes, (b) at 15 minutes. N_2^+ peak (c) at 5 minutes, (d) at 15 minutes.

S.5 Electronic temperature calculation **S10**

Text S1 Electronic temperature calculation.

S.6 Analyze of plasma discharge power **S11**

Text S2 Calculation of plasma discharge power.

Fig. S16 Lissajous diagram in plasma discharges.

Fig. S17 Voltage-current (U-I) waveforms with different TiO_2 additions.

S.7 Isotope labelling experiments **S13**

Text S3 Isotope labelling experimental procedure.

Fig. S18 Photograph of the PACL system used for isotope labelling experiments.

S.8 Comparison with NH_3 synthesis rates reported in the literature **S14**

Tab. S5 Comparison of ammonia production rates for low-temperature nitrogen fixation systems.

S.1 Analysis of Plasma Discharge Temperature Characteristics

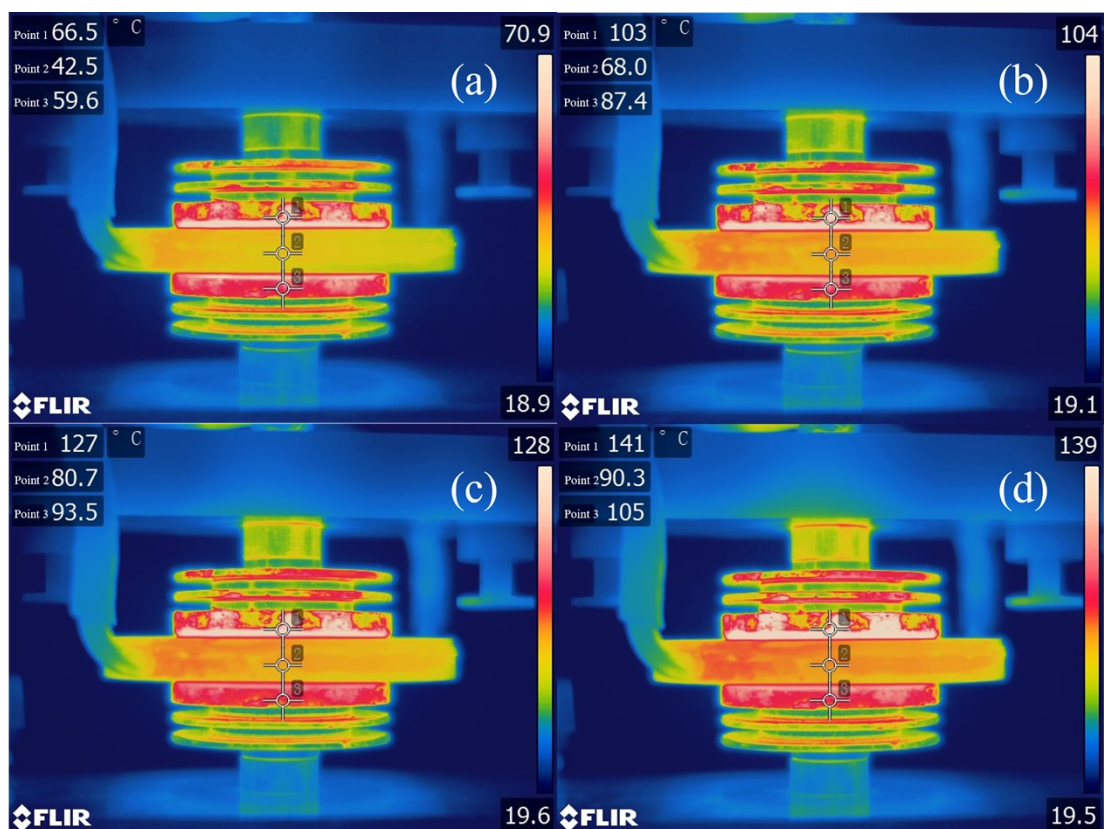


Figure S1 Thermal imaging diagram of the reactor during the 97%-TiMgO plasma nitrogen fixation process: a at the 5th minute, b at the 10th minute, c at the 15th minute, d at the 20th minute.

S.2 Thermodynamic calculation

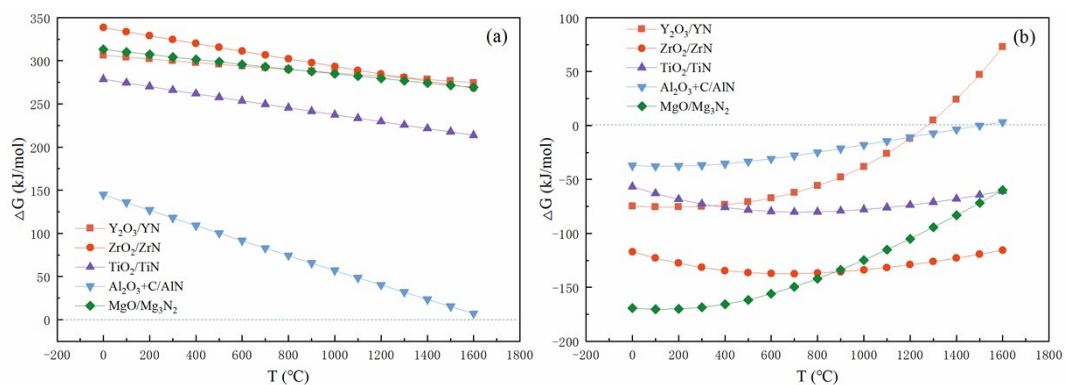


Figure S2 ΔG variation with temperature. (a) Nitrogen fixation reaction, (b) Nitrogen release reaction.

Table S1 Comparison of hydrolysis characteristics of metal nitrides.

Metal nitrides	NH_3 yield ($\mu\text{mol g}^{-1}$)	Error bar
Mg_3N_2	4896.61882	238.97524
TiN	9.95181	0.04076

S.3 Characterization analysis

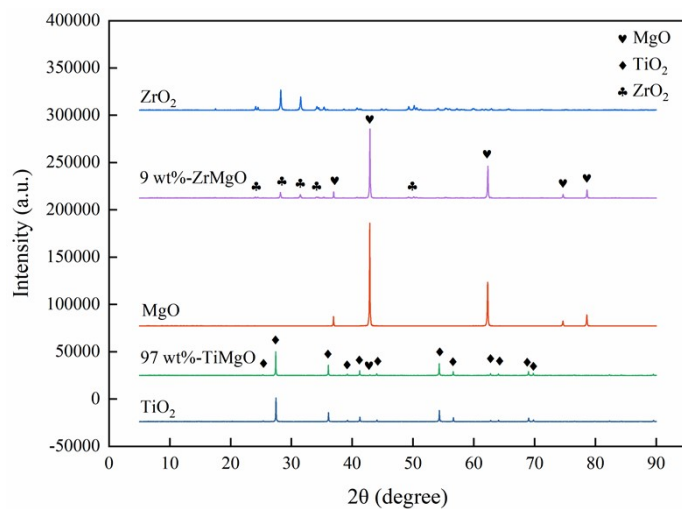


Figure S3 XRD patterns of the MO_x before the reaction.

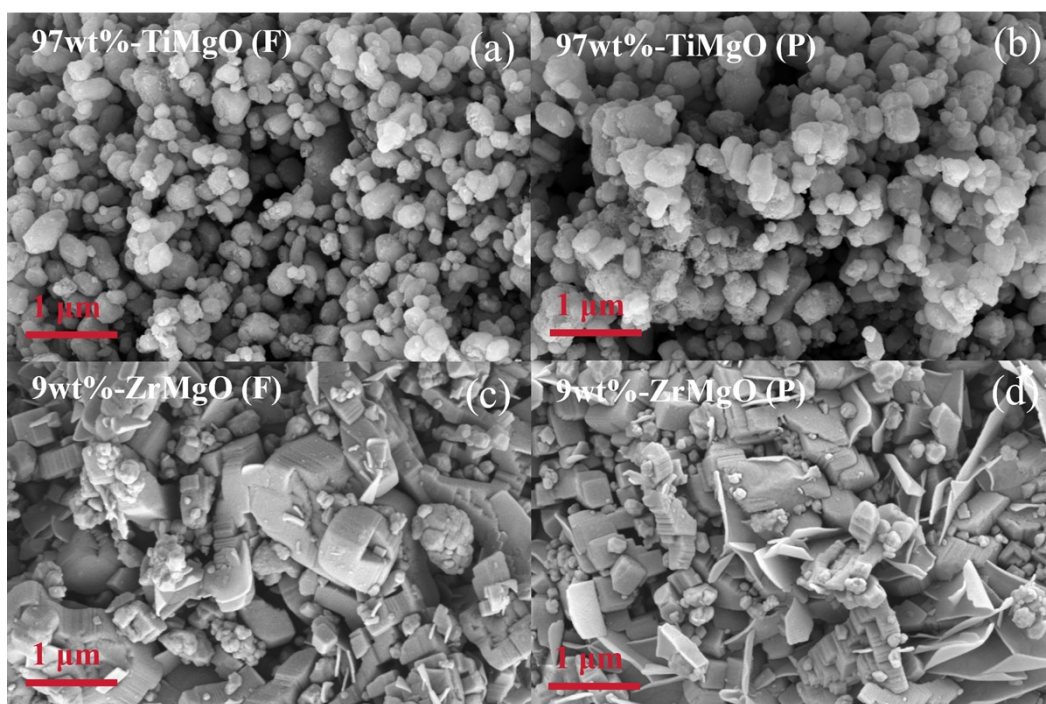


Figure S4. SEM images of (a) 97wt%-TiMgO (F), (b) 97wt%-TiMgO (P), (c) 9wt%-ZrMgO (F), (d) 9wt%-ZrMgO (P). Scale bars: 1 μm. F and P denote fresh and post-reaction samples, respectively.

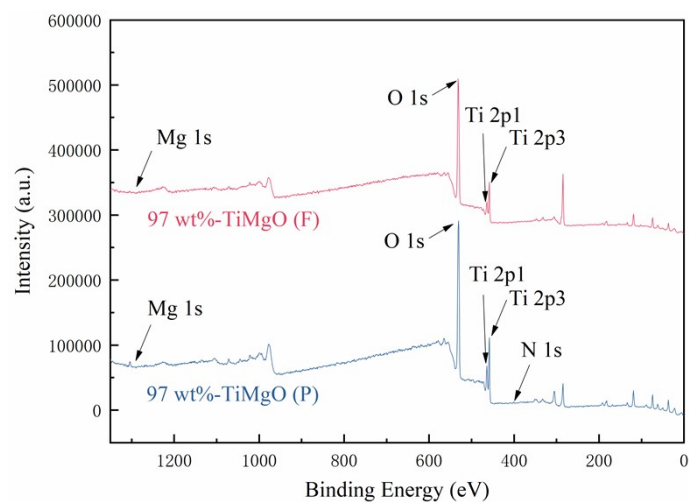


Figure S5. XPS full spectra of 9 wt%-TiMgO and 97 wt%-TiMgO.

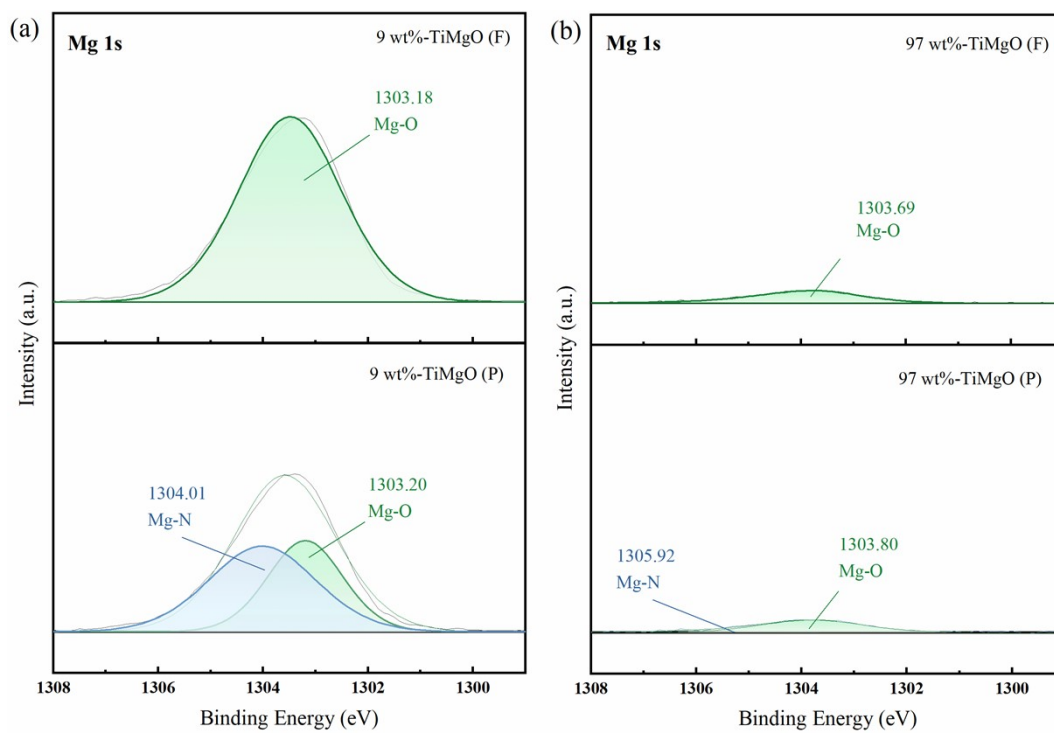


Figure S6. Mg 1s spectra of (a) 9 wt%-TiMgO, (b) 97 wt%-TiMgO.

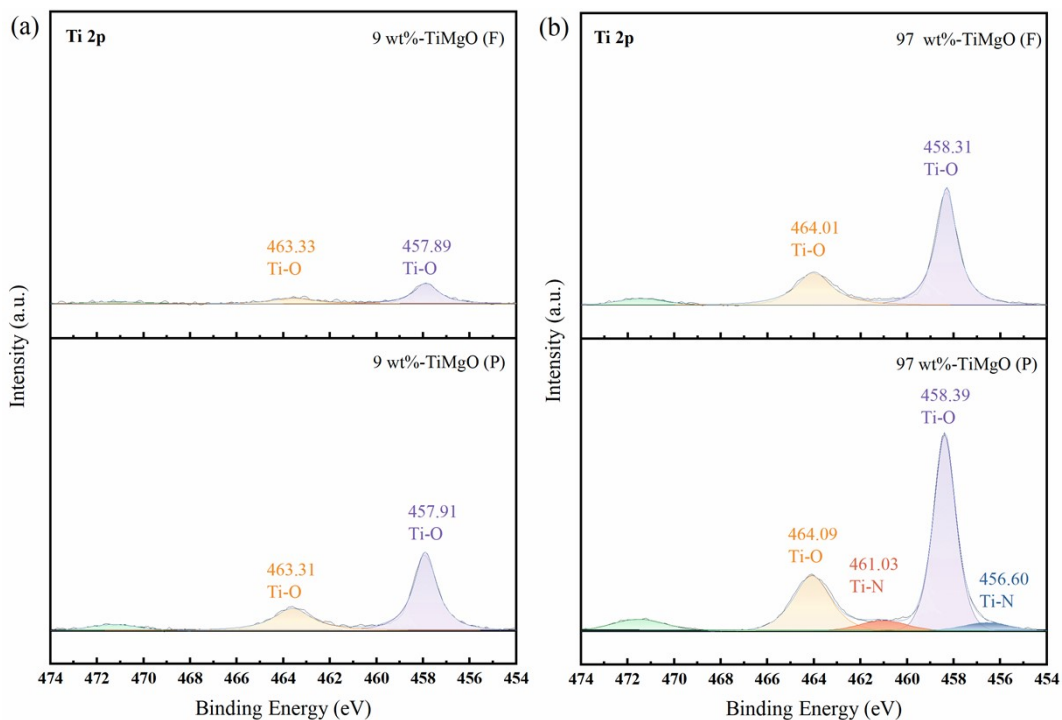


Figure S7. Ti 2p spectra of (a) 9 wt%-TiMgO, (b) 97 wt%-TiMgO.

Table S2. XPS N 1s quantification of nitrogen species during F (fresh), P (plasma-nitrided), and H (hydrolyzed) stages.

Sample	F (N at%)	P (N at%)	H (N at%)	Nitridated N (N at%) (P-F)	Hydrolyzed N (N at%) (P-H)	Hydrolysis Efficiency (%)
9 wt%-TiMgO	0%	0.36%	0.09%	0.36%	0.27%	75%
97 wt%-TiMgO	0.47 %	1.58%	0.84%	1.11%	0.74%	67%

Note: Nitridated N was the fixed nitrogen by plasma treated calculated through the XPS N at%, Hydrolyzed N represents the reduction in the XPS N at% of solid substances before and after the hydrolysis reaction of metal nitrides. The hydrolysis efficiency was calculated as the ratio of the decreased XPS N at% of the solid sample after hydrolysis to the increased XPS N at% induced by plasma-mediated nitrogen fixation. The detailed formula is provided in Eq. S1-3.

$$N_{\text{Nitridation}} = N \text{ at\%}(P) - N \text{ at\%}(F) \quad (\text{S-1})$$

$$N_{\text{Hydrogenation}} = N \text{ at\%}(P) - N \text{ at\%}(H) \quad (\text{S-2})$$

$$\text{Efficiency}_{\text{Hydrogenation}} = \frac{N_{\text{Nitridation}}}{N_{\text{Hydrogenation}}} \times 100\% \quad (\text{S-3})$$

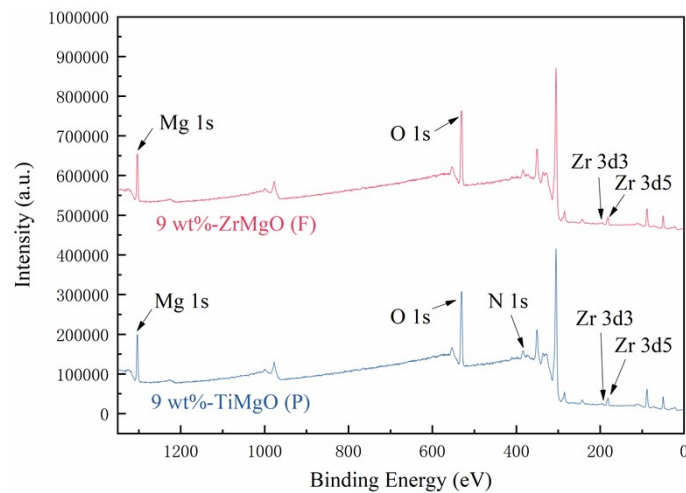


Figure S8. XPS full spectra of 9 wt%-ZrMgO and 97 wt%-ZrMgO

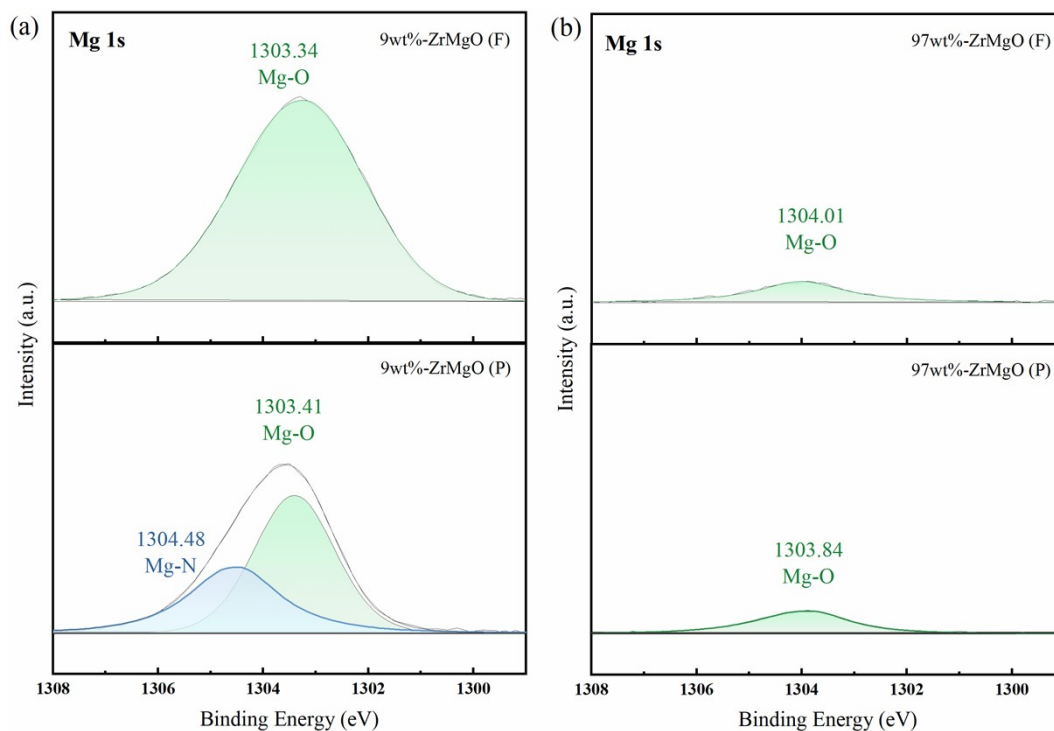


Figure S9. Mg 1s spectra of (a) 9 wt%-ZrMgO, (b) 97 wt%-ZrMgO.

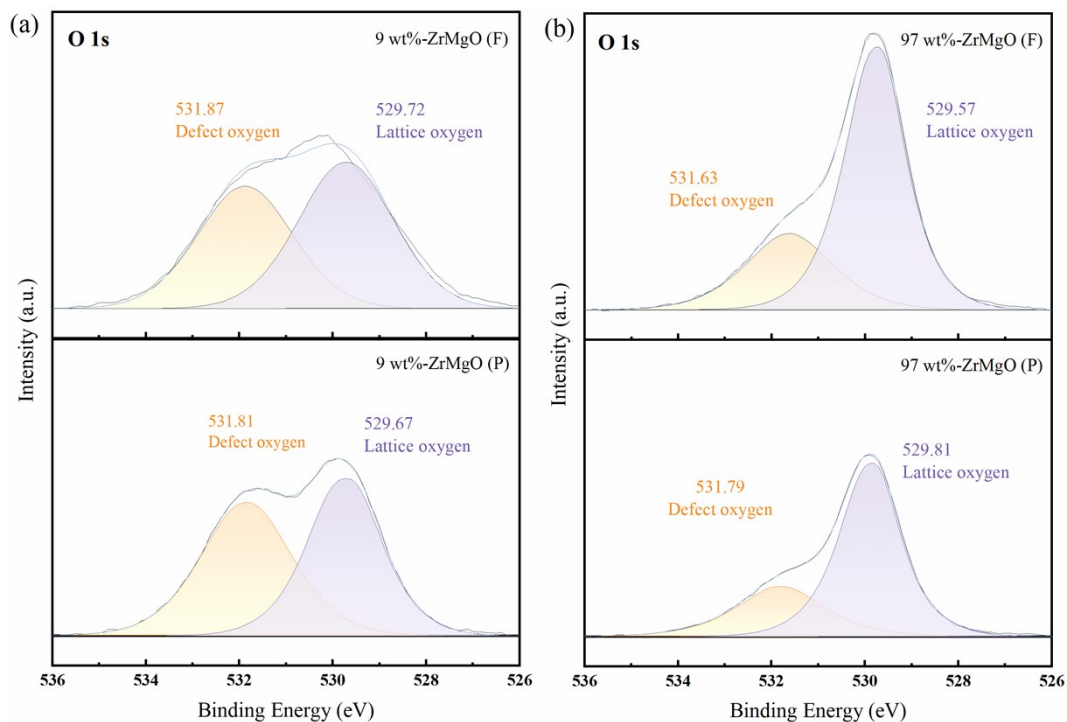


Figure S10. O 1s spectra of (a) 9 wt%-ZrMgO, (b) 97 wt%-ZrMgO.

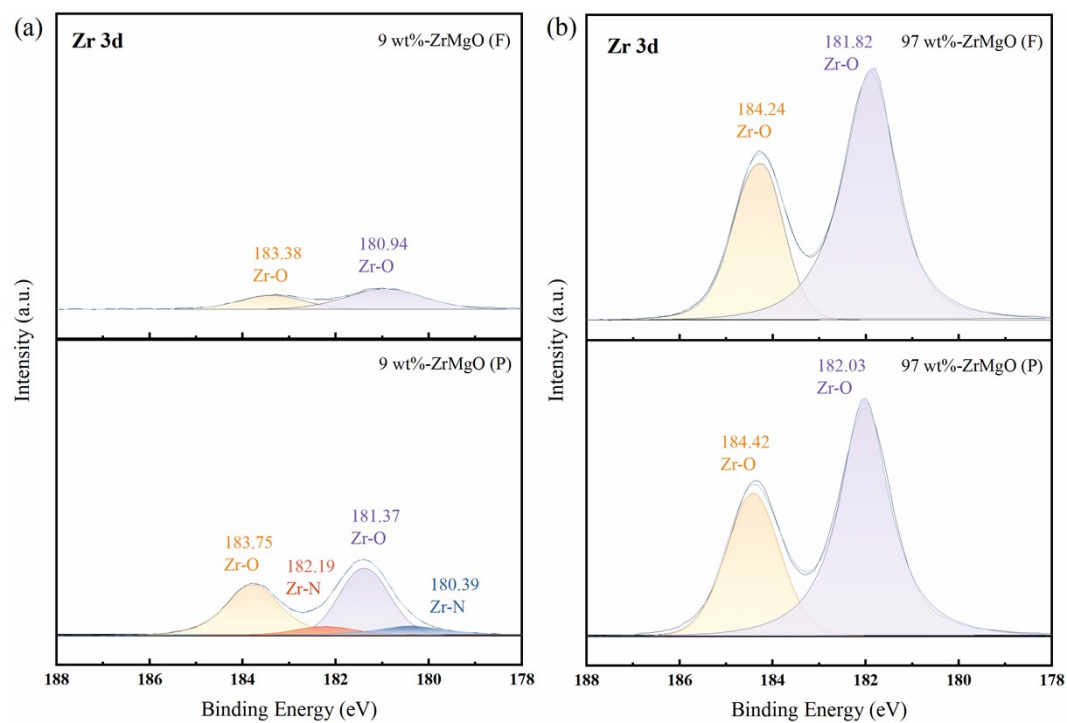


Figure S11. Zr 3d spectra of (a) 9 wt%-ZrMgO, (b) 97 wt%-ZrMgO.

Table S3. Surface elemental distribution of 9 wt %-ZrMgO(P) (EDS mapping results)

Element	Line type	Apparent concentration	k-Ratio	Wt%	Wt% sigma
N	K	0.34	0.00234	0.99	0.24
O	K	12.44	0.10901	29.30	0.22
Mg	K	42.19	0.38810	52.15	0.30
Zr	L	11.22	0.11216	17.56	0.37

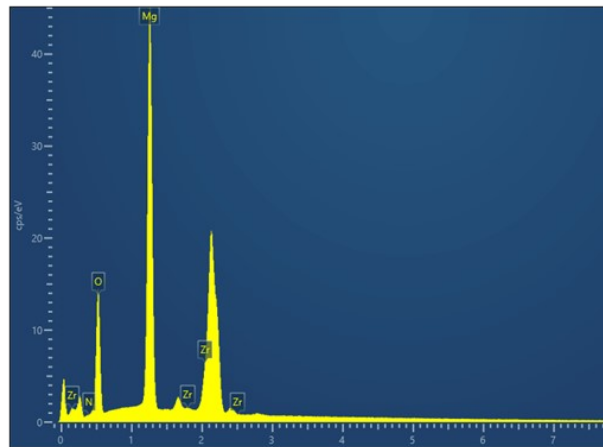


Figure S12. Total number of elemental distribution spectra for 9 wt%-ZrMgO (P)

Table S4. Surface elemental distribution of 9 wt %-ZrMgO(P)
(EDS spot scanning results)

Surface region	Element	Line type	Apparent concentration	k-Ratio	Wt%
Spot 1	N	K	0.60	0.00416	2.04
Spot 2	N	K	0.46	0.00316	1.44

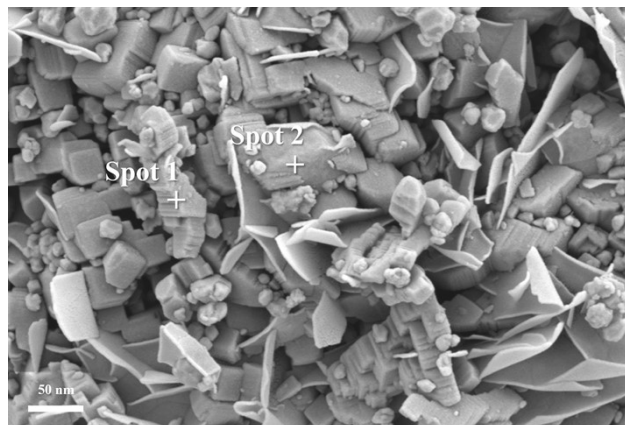


Figure S13. EDS spot scanning of 9 wt%-ZrMgO

S.4 Plasma spectral analysis

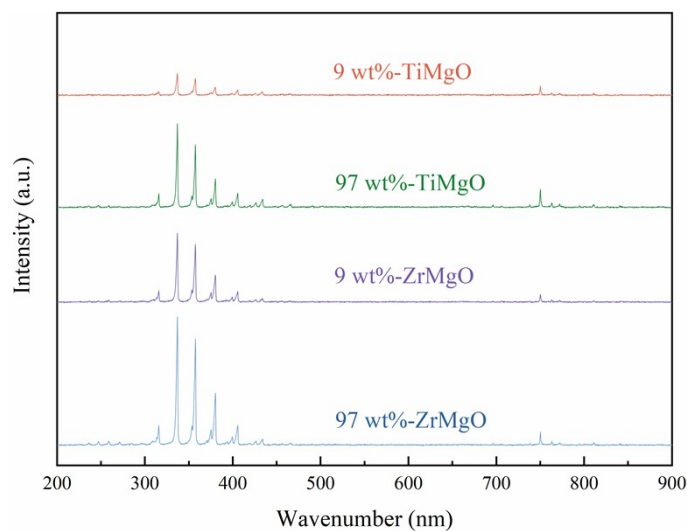


Figure S14. OES spectra of MO_x after 15 min treatment

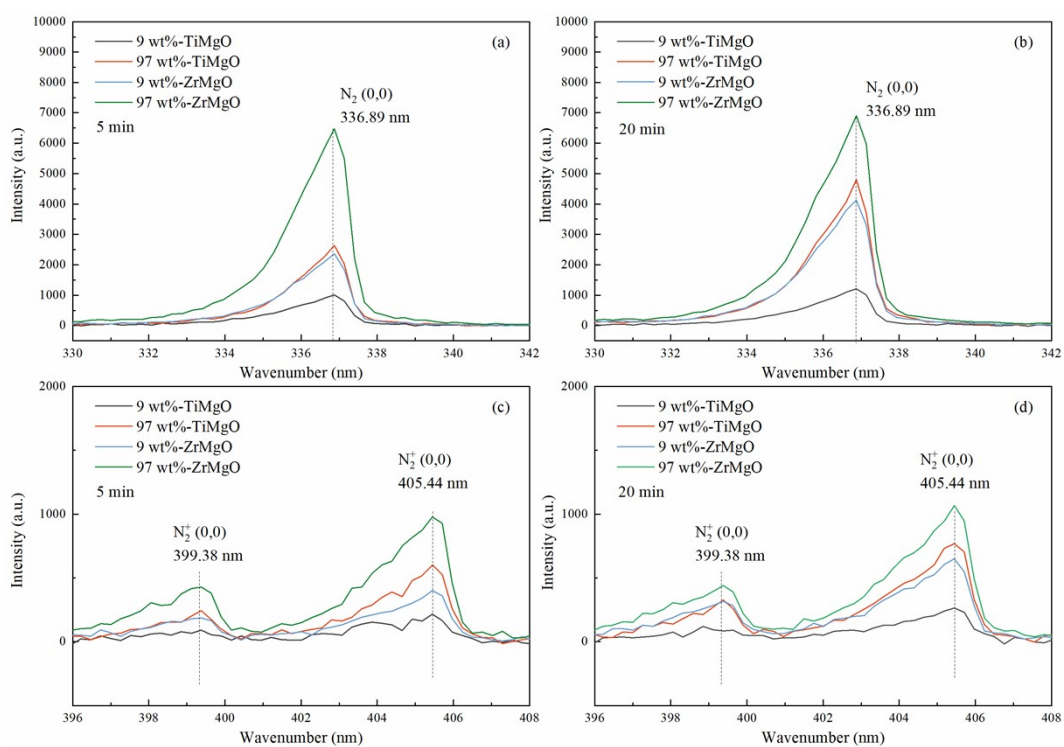


Figure S15. N_2 bands (a) at 5 minutes, (b) at 15 minutes. N_2^+ bands (c) at 5 minutes, (d) at 15 minutes.

S.5 Electronic temperature calculation

Text S1 Electronic temperature calculation.

The Boltzmann method is employed to calculate the electron excitation temperature (T_{exc}) from the emission spectrum. For a given vibrational line, the following relationship holds as Eq. S4:

$$\ln\left(\frac{I\lambda}{gA}\right) = \ln D - \frac{E_u}{k_B T_{\text{exc}}}, \quad (\text{S-4})$$

Where: I denotes spectral line intensity, λ denotes corresponding wavelength, g denotes statistical weighting, A denotes transition probability, E_u denotes the transition energy level, k_B represents the Boltzmann constant, T_{exc} signifies the electron excitation temperature, $D = N_S(T)/U_S(T)$, where D is a constant, $N_S(T)$ denotes the total particle number density, and $U_S(T)$ represents the partition function. The required transition parameters for the equation were obtained from the NIST database. Linear fitting was performed using Ar lines at 357.32, 380.09, 705.44, and 800.72 nm. Data points were fitted with $\ln(I\lambda/gA)$ on the y-axis and transition energy level E_u on the x-axis. T_{exc} can be calculated by the slope of $-1/k_B T_{\text{exc}}$.

S.6 Analyze of plasma discharge power

Text S2 Calculation of plasma discharge power.

A high-voltage probe was used to detect the reactor's real-time output power, with the incorporated internal capacitor in the power supply to determine the charge accumulated in the DBD. Based on oscilloscope detection of the output sine wave, a Lissajous figure was obtained and the area can be calculated, as referenced in Fig. S16. The discharge power P (W) of the reactor used in the experiment can be expressed by Eq. S5:

$$P = f \times C \times A \quad (\text{S-5})$$

Where f (Hz) denotes frequency, C (F) represents the measured capacitance ($C = 0.47 \mu\text{F}$), and A signifies the area of the Lissajous figure.

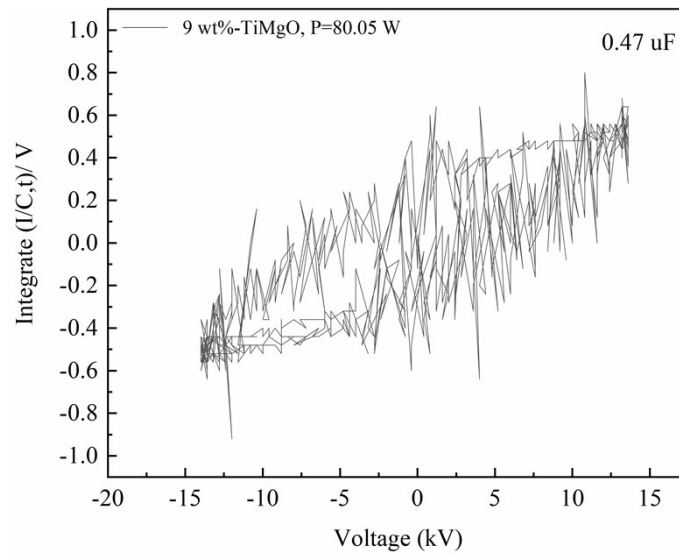


Figure S16. Lissajous diagram in plasma discharges.

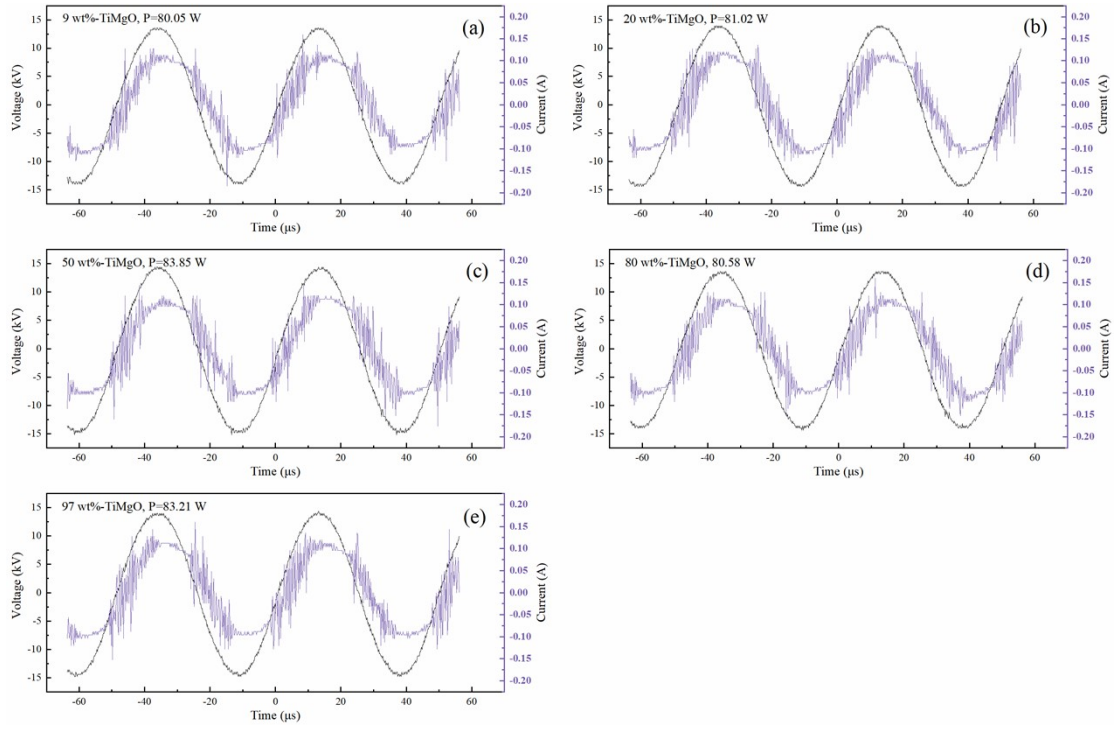


Figure S17. Voltage-current (U-I) waveforms with different TiO_2 additions: (a) 9 wt%-TiMgO, (b) 20 wt%-TiMgO, (c) 50 wt%-TiMgO, (d) 80 wt%-TiMgO, (e) 97 wt%-TiMgO.

S.7 Isotope labelling experiments.

Text S3. Isotope labelling experimental procedure:

To further identify the nitrogen source for NH_3 production, isotope labelling experiments were conducted on the 97 wt%-TiMgO samples. The experimental procedure is shown in Figure S18. The apparatus was purged with 50 mL min^{-1} of Argon for 10 minutes to ensure the absence of residual air. The gas in the experimental chamber was then switched, with Ar, $^{14}\text{N}_2$ and $^{15}\text{N}_2$ (99.9%, Amber Bridge Advanced Materials & Tech Co., Ltd) each being used at a flow rate of 20 mL min^{-1} for a 10-minute purge, after which the inlet and outlet valves were closed. A 20-minute sealed plasma discharge experiment was then conducted. Subsequently, 0.5 g of the MN_x was hydrolysed in 5 mL of water at 80°C for 120 minutes. The supernatant (0.5 mL) was then mixed with HCl (1 M, $50 \mu\text{L}$) and DMSO-d 6 ($25 \mu\text{L}$). The resulting solution was transferred to a tube for NMR measurement. The NH_3 concentration was determined using a Bruker 600 MHz NMR spectrometer.

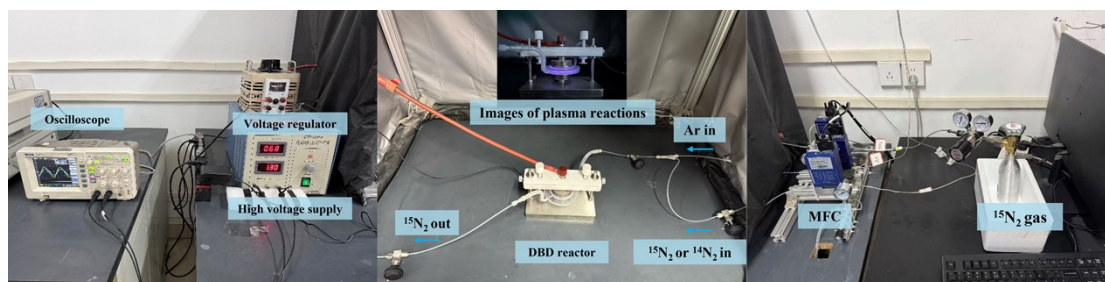


Figure S18 Photograph of the PAEL system used for isotope labelling experiments.

S.8 Comparison with NH₃ synthesis rates reported in the literature.

Table S5 Comparison of ammonia production rates for low-temperature nitrogen fixation systems.

Nitrogen carrier/Catalyst	Method	Temperature	NH ₃ production rate	Ref.
97 wt%-TiMgO	N ₂ and H ₂ O PACL	<100 °C (T _P =20 min)	1.83 μmol g ⁻¹ h ⁻¹ (T _H =20 min) 0.95 μmol g ⁻¹ h ⁻¹ (T _H =120 min)	This work
MgO	N ₂ and H ₂ O PACL	200 °C (T _P =10 min)	1.49 μmol g ⁻¹ h ⁻¹ (T _H =10 min)	1
Li-Zn alloy and LiCl-KCl salt	N ₂ and H ₂ catalysis	400 °C (T _R =2 h)	0.15 μmol g ⁻¹ h ⁻¹ (T _R =2 h)	2
TiN/MgO	N ₂ and H ₂ O photocatalytic PACL	550 °C (T _R =14 h)	1.67 μmol g ⁻¹ h ⁻¹ (T _R =14 h)	3

T_P : Plasma nitrated time;

T_H : Hydrolyzed time.

T_R: One-Step Ammonia Synthesis reaction time.

NH₃ synthesis rate:

$$R_{\text{NH}_3} = \frac{Y_{\text{NH}_3}}{T_{\text{Nitridation}} + T_{\text{Hydrogenation}}} \quad (\text{S-6})$$

R_{NH_3} denotes the NH₃ production rate, $T_{\text{Nitridation}}$ denotes the nitrogen fixation time, and $T_{\text{Hydrogenation}}$ denotes the hydrolysis time. In this study, the highest NH₃ production rate was 2.23 μmol g⁻¹ (hydrolysis for 120 min) and 1.22 μmol g⁻¹ (hydrolysis for 20 min). After conversion, the NH₃ production rates were 1.83 μmol g⁻¹ h⁻¹ and 0.95 μmol g⁻¹ h⁻¹.

References:

1. S. Zen, T. Abe and Y. Teramoto, *PLASMA CHEMISTRY AND PLASMA PROCESSING*, 2018, **38**, 347-354.
2. X. Meng, J. Liu, Z. Tang, B. Xi, P. Yan, X. Wang, K. Cao, B. Yang and X. Guan, *Catalysis Science & Technology*, 2024, **14**, 3320-3334.
3. D. F. Swearer, N. R. Knowles, H. O. Everitt and N. J. Halas, *ACS Energy Letters*, 2019, **4**, 1505-1512.